

## A Robust Finger Knuckle Print Authentication using Topothesy and Fractal Dimension

Madasu Hanmandlu\*, Neha Mittal#, and Ritu Vijay<sup>1</sup>

\*Electrical Engineering Department, Indian Institute of Technology Delhi, New Delhi - 110 016, India

#Electronics Engineering Department, JP Institute of Engineering and Technology, Meerut - 250 001, India

<sup>1</sup>Electronics Department, Banasthali University, Banasthali - 304 022, India

\*E-mail: mhmandlu@ee.iitd.ac.in

### ABSTRACT

The finger knuckle based biometric authentication system using the approaches like, Gaussian smoothed high pass, Gaussian smoothed oriented derivative, and also the well known method for surface roughness measurement called the fractal profiles represented by Topothesy and fractal dimension which describe not only the roughness but also the affine self similarity is presented. Daisy descriptor for the representation of texture implemented. The results of fractal parameters along with the refined scores are comparable to those of the compcode and impcompcode.

**Keywords:** Finger-knuckle-print; Gaussian smoothed high pass; Gaussian smoothed oriented derivative; Structure function; Fractal parameters; Score level fusion; Refined scores method

### 1. INTRODUCTION

The finger-knuckle-print (FKP) based recognition system is gaining momentum ever since the work of Zhang<sup>1</sup>, *et al.* who have developed an acquisition system to capture the FKP. After cropping the region of interest (ROI), a competitive coding scheme is employed to extract the FKP features. FKP based recognition scheme is also presented by Zhang<sup>2</sup>, *et al.*. The FKP images are acquired by a specific data acquisition device. Orientation and magnitude information are extracted by the Gabor filter. This system has high recognition accuracy and works in real time. An effective FKP authentication system is developed by Zhang<sup>3</sup>, *et al.*. They have extracted an ensemble of local and global features of FKP. The local features constitute the orientation information extracted using the Gabor filters based on the competitive coding scheme. When scale of the Gabor transform tends to infinity, it degenerates into the Fourier transform from the viewpoint of time-frequency analysis. Global features are the Fourier transform coefficients of an image. Combining local and global information improves the recognition accuracy as compared to that due to either local or global information.

Zhang<sup>4</sup>, *et al.* have investigated the image local features using the phase congruency model that supports the psycho-physical and neuro-physiological evidences for FKP recognition. The local orientation and local phase are extracted from a local image patch while computing the phase congruency. These local features are independent of each other

and represent diverse aspects of image local information. The three local features are computed under the framework of phase congruency using a set of quadrature pair filters. These three local features are integrated at score level fusion to improve FKP recognition accuracy. Such local features can also be naturally combined with Fourier transform coefficients, which are global features.

Morales<sup>5</sup>, *et al.* have presented a new approach for the verification of FKPs of a person. Gabor filter is applied to enhance FKP information and a scale invariant feature transform (SIFT) to extract features. The SIFT features obtained after Gabor enhancement of principal finger knuckle lines improve the performance of the verification system. Zhu<sup>6</sup> has presented SURF based knuckle print recognition system. Random sample consensus (RANSAC) has been utilised to establish the geometric constraint to remove false matching.

Zahra<sup>7</sup>, *et al.* have used both the intensity and Gabor features of each FKP. The best recognition performance is obtained when the features of all fingers are used.

An attempt is made here to explore the effectiveness of fractal parameters comprising Topothesy and fractal dimension for the representation of FKP texture using the structure function. Topothesy deals with the roughness property whereas fractals are self-similar on multiple scales, and have a fractional dimension<sup>8</sup>. Another motivation is to make use of the orientation information just as competitive coding by devising new features.

## 1.1 Finger Knuckle Database

The FKP database used here is taken from Polytechnic University, Hong Kong<sup>9</sup>. This database contains 165 users, 4 FKPs for each user and 6 images for each FKP, totaling 3960(165x4x6) images from 660 fingers in the first session. The FKPs consisting of left index, left middle, right index and right middle of a user are as shown in Figs. 1(a) - 1(d).

## 2. FEATURE EXTRACTION

### 2.1 Gaussian Smoothed High Pass Response

We have devised a new feature which is the sum of the differences of the current pixel intensity and its mxm neighbouring pixels. The sum of (mxm-1) differences is given by:

$$s = \sum_{\substack{i=1 \\ i \neq (m+1)/2}}^m \sum_{\substack{j=1 \\ j \neq (m+1)/2}}^m \left( I\left(\frac{m+1}{2}, \frac{m+1}{2}\right) - I(i, j) \right) \quad (1)$$

To express the computation in Eqn. (1) we define mask  $w$  for  $m = 5$  as

$$w = \begin{bmatrix} -1 & -1 & -1 & -1 & -1 \\ -1 & -1 & -1 & -1 & -1 \\ -1 & -1 & 24 & -1 & -1 \\ -1 & -1 & -1 & -1 & -1 \\ -1 & -1 & -1 & -1 & -1 \end{bmatrix}$$

Then the computation in Eqn. (1) is represented by the convolution of the image  $I(x, y)$  with the mask given by

$$S = I(x, y) * w \quad (2)$$

where the size of  $I$  is  $M \times N$ , the size of  $w$  is  $m \times n$ , and the size of  $S$  is  $(M-(m-1)) \times (N-(n-1))$ . The above convolution is expressed mathematically as,

$$s(x, y) = \sum_{p=-a}^a \sum_{q=-b}^b w(p, q) I(x+p, y+q)$$

$a = (m-1)/2$  and  $b = (n-1)/2$  for  $x = 0, 1, 2, \dots, M-1$  and  $y = 0, 1, 2, \dots, N-1$ . Next  $s$  is convolved with the Gaussian function  $G$  to give  $S_f = S * G$  (3)

where  $G$  is defined as

$$G = \frac{1}{2\pi\sigma^2} e^{-\frac{x^2+y^2}{2\sigma^2}}$$

The value of  $\sigma$  is set to 0.4 after experimentation. The size of  $S$  is  $(M-m-1) \times (N-n-1)$  and the size of  $G$  is taken as  $axa$ . The size of  $S_f$  is obtained as  $(M-(m-1)-(a-1)) \times (N-(n-1)-(a-1))$ , where  $m = n = 5$  and  $a = 7$ . Here the size of  $I$  is  $(55 \times 110)$  and the size of  $S_f$  is  $(55-4-6=45, 110-4-6=100)$ .

The first convolution in Eqn. (2) modifies the original image into an image of differences and the second convolution in Eqn. (3) converts these differences into information values, which are products of the information source values, i.e.  $s$  values

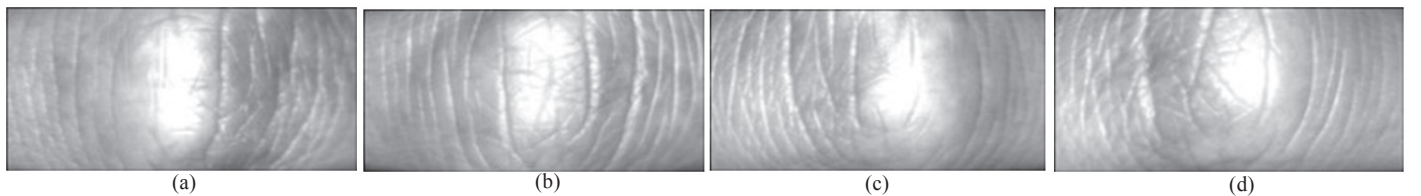


Figure 1. FKP of (a) Left index, (b) Left middle, (c) Right index and (d) Right middle.

and the Gaussian membership function values. The concept of information set and information values can be found in Mamta and Hanmandlu<sup>10</sup> and this concept is not explored here.

### 2.2 Gaussian Smoothed Oriented Derivatives

To compute the horizontal and vertical gradients, we perform two 1D convolutions with differentiation kernels  $[-1 \ 1]$  and  $[-1 \ 1]^T$ , respectively. The resulting horizontal and vertical gradients are denoted by  $I'_x$  and  $I'_y$  which are the approximations of the horizontal and vertical gradients. The overall direction of these two gradients at the location  $(x, y)$  is computed as

$$G_\theta = \max(I'_x \cos \theta + I'_y \sin \theta, 0) \quad (4)$$

This gradient image  $G_\theta$  is convolved with the Gaussian function  $G$  in Eqn. (3) to yield GSOD denoted by  $G_{OD}$ . The GSOD feature representation on FKPs is depicted in Fig. 2 in the form of intensity image at orientations of  $30^\circ, 60^\circ, 90^\circ, 120^\circ$ , and  $150^\circ, 180^\circ$  from left to right and from top to bottom, respectively. Thus we have six images corresponding to 6 orientations.

The size of  $I$  is  $(M \times N)$ ,  $G_\theta$  is  $(M-1) \times (N-1)$  and the size of  $G$  is taken as  $axa$ . The size of  $G_{OD}$  is obtained as  $(M-1-(a-1)) \times (N-1-(a-1))$ , where  $a = 7$ . Here the size of  $I$  is  $(55 \times 110)$  and the size of  $G_{OD}$  is  $(55-1-6=48, 110-1-6=103)$ .

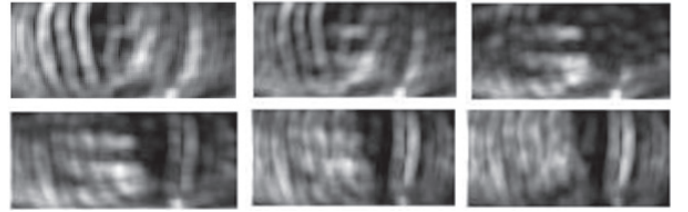


Figure 2. Response of the GSOD in six orientations ( $30^\circ, 60^\circ, 90^\circ, 120^\circ, 150^\circ$  and  $180^\circ$ ).

### 2.3 Fractal Parameters

Our focus is on FKP textures which are random and irregular. In this work, fractal based approaches are investigated for the analysis of finger knuckle print for personal authentication. Fractals exhibit self-similarity, i.e. the whole structure is approximately similar in shape to its constituent parts. The traditional approaches like Box-Counting are already used for the computation of fractal dimension by Chaudhuri and Sarkar<sup>11</sup>. Fractal profiles to be investigated for the representation of FXP texture are not only self similar but also self-affine. In such profiles, their self affinity may be represented by an additional measure called topothesy<sup>12</sup>. The fractal profiles are characterised by two parameters called fractal parameters: Fractal dimension and topothesy.

#### 2.3.1 The Structure Function

The motivation for the structure function stems from the

work of Hanmandlu<sup>13</sup>, *et al.* A brief description of structure function is in order. The structure function is a measure of the frequency variation in a signal caused by the change in the roughness and it bears a relation with the fractal parameters. The structure function (SF) for a particular 1-D (one dimensional) discrete function  $z(x)$  and for a particular value of delay  $\tau$  ( $\tau \in \mathbb{Z}$ ,  $1 < \tau < m$ ),  $m$  being the number of data points available, is expressed as

$$S(\tau) = \frac{1}{m - \tau} \sum_{i=1}^{m-\tau} |z(i) - z(i + \tau)| \quad (5)$$

As the images involve two dimensions  $\tau_x$  and  $\tau_y$ , the structure function in 1-D is changed to 2-D (two dimensional) as:

$$S(\tau_x, \tau_y) = \frac{1}{(m - \tau_x)(n - \tau_y)} \sum_{i=1}^{m-\tau_x} \sum_{j=1}^{n-\tau_y} |z(i, j) - z(i + \tau_x, j + \tau_y)| \quad (6)$$

where the size of the sub image is (mxn). Referring to Eqn. (6), it may be noted that the change in the intensity values in two windows separated by  $\tau_x = \tau_y = \tau$  gives a measure of roughness whereas the change in the intensities over several values of  $\tau$  possess self-similarity. Thus both roughness and self-similarity are accounted for in Eqn. (6).

As the SF bears a relation with the fractal parameters, we will examine its mathematical expression in Eqn. (6). The SF is also a function of the fractal parameters as given by:

$$s(\tau) = \Lambda^{(2D-2)} \tau^{2(2-D)} \quad (7)$$

In this study, we estimate the asymptote by the best line fit passing through the initial and the end points of the hyperbola. The asymptote is evaluated by taking log of Eqn. (6) which leads to

$$\begin{aligned} \log s(\tau) &= (2D - 2) \log \Lambda + 2(2 - D) \log \tau \\ &= \text{Intercept} + \text{slope} * \log \tau \end{aligned} \quad (8)$$

The y-intercepts and slopes of the two tangents drawn on the hyperbola can be used to find the fractal dimension  $D$  and toposy  $\Lambda$  from Eqn. (8). The first term in Eqn. (8) gives the property of self-similarity whereas the second term gives the property of roughness. Thus  $D$  is derived from

$$\text{slope} = 2(2 - D) \quad \text{as} \quad D = \frac{4 - \text{slope}}{2} \quad (9)$$

and  $\Lambda$  from the intercept  $= (2D-2)\log\Lambda$  of the logarithmic plot as

$$\Lambda = \text{anti log} \left( \frac{\text{Intercept}}{(2D - 2)} \right) \quad (10)$$

Knowing the values of both slope and intercept from the asymptote, the parameters  $D$  and  $\Lambda$  can be computed for all the windows.

**Algorithm for the Extraction of Fractal parameters**

- (a) Slide the subimage of size mxn (taken as 5x5, 6x6 and 7x7) through the image of size MxN.
- (b) For each sub-image, repeat Steps (c) to (f) until all sub images are exhausted.
- (c) Calculate SF as a function of  $\tau_x$  and  $\tau_y$  using Eqn (6), for each value of  $\tau_x, \tau_y$  ranging from 1 to m-1, n-1 respectively.
- (d) Take the logarithmic of SF for each value of  $\tau_{xy}$ .

- (e) Fit a parabola using the points  $(\log(\tau_x, \tau_y), \log(S(\tau_x, \tau_y)))$ .
- (f) Draw two tangents to the parabola and use these to find the fractal dimension  $D$  and Topothesy  $\Lambda$  for the sub image under consideration as given in Eqns. (9) and (10).
- (g) Obtain the toposy and fractal dimension features corresponding to each subimage.

Note that for each sub image, we obtain a structure function from which we compute toposy and fractal dimension. Thus we get two features for each sub image thus leading to two feature matrices one for the toposy and another for fractal dimension. These feature matrices are of size:  $(M-(m-1), N-(n-1))$  corresponding to FKPs of size MxN and sub image of size mxn.

**2.4 FKP Matching based on Feature Matrices**

In the case of DAISY descriptor the FKP features are in the vector form. Let  $P_v$  and  $Q_v$  be the two feature vectors corresponding to training and test samples respectively. Then we use the Euclidean distance  $d(P_v, Q_v)$  between these two feature vectors for matching.

The computation of GHSP and GSOD involving convolution operations is turned out to be feature matrices. Also toposy and fractal dimension features are also in matrix form. Hence FKP matching is matrix based. Let  $P_m$  and  $Q_m$  be two feature matrices corresponding to training and test samples, then the matching distance between them is defined as:

$$D(P_m, Q_m) = \frac{\sum_{x=1}^{\text{rows}} \sum_{y=1}^{\text{cols}} \text{abs}(P_m(x, y) - Q_m(x, y))}{A} \quad (11)$$

where A is the overlapping area of two feature matrices with x and y denoting the row and column numbers respectively. The possible translation of region of interest (ROI) of FKP has been taken into account during matching.

Zhang<sup>2</sup>, *et al.* perform multiple matches by translating one set of features in both horizontal and vertical directions. The minimum matching distance from all the translations is considered as the final score. The ranges of horizontal and the vertical translations are empirically set as -8 to 8 and -4 to 4, respectively.

**2.5 The method of Refined Scores**

To match the given query with the claimed identity, Mamta and Hanmandlu<sup>10</sup> used the information of the neighbours to refine the decision of selection or rejection of a user. In the conventional case, if the scores are less than the predefined threshold, then the user is classified as the genuine, otherwise an imposter. Because of the corrupted data, there is a decrease in the intraclass similarity and an increase in the interclass similarity. As a result the genuine and imposter scores are overlapped leading to wrong decision. By this, some genuine users get falsely rejected (FRR) while some imposters falsely accepted (FAR). In such cases, the scores are refined by applying rechecks on the error scores.

The performance metrics of biometric system are defined as follows:

*False Acceptance Rate (FAR)* is the ratio of the number of imposters (unauthorised users) being accepted to the total

number of users registered in the system.

$$FAR = \frac{\text{Number of imposters falsely accepted}}{\text{Number of imposter recognition attempts}}$$

False Rejection Rate (FRR) is the ratio of the number of genuine (authorised users) being rejected to the total number of users registered in the system.

$$FRR = \frac{\text{Number of genuine falsely rejected}}{\text{Number of genuine recognition attempts}}$$

Genuine Acceptance Rate (GAR) is defined as  $GAR = 1 - FRR$ .

Equal Error Rate (EER) is the rate at which both FAR and FRR are equal.

Receiver Operating Characteristic (ROC) is a plot of GAR along the Y-axis vs. FAR along the X-axis and it is used to evaluate the performance of a biometric system.

## 2.6 Improvement of FRRs and FARs

To improve FRR, if a score is more than the threshold ( $T$ ) instead of rejecting it is refined using the cohort information provided by the neighbours of the claimed identity. Let  $X^q$  be the query sample and  $X_{Cl}^r$  be the claimed sample. Let  $d = ED(X^q, X_{Cl}^r)$  be the matching score computed as the Euclidean distance ( $ED$ ) between the query sample and the claimed sample  $X_{Cl}^r$  such that

$$ED(X^q, X_{Cl}^r) = \begin{cases} Gen, & \text{if } d < T \\ Im, & \text{if } d > T \end{cases} \quad (12)$$

where  $T$  is the threshold. If ( $d < t$ ) then the matching score is claimed as the genuine ( $Gen$ ) otherwise imposter ( $Im$ ). For example if  $N$  is the number of users then we will have only  $N$  genuine matching scores but  $N \times (N-1)$  imposter matching scores. This means that almost all bins in the knowledge database will be occupied by the imposter matching scores, only a small proportion is occupied by the genuine matching scores. So we utilise the neighbourhood samples of the claimed sample to generate the neighbourhood score which is the Euclidean distance between the query sample and the neighbourhood sample.

If the matching score is above the threshold then it is rechecked with all the neighbourhood scores of the claimed score of that user. If any of the neighbourhood score is less than the matching score then the claimed user is said to be imposter but if the matching score is less than all of the neighbourhood scores then the user is authenticated as the genuine. The rejection rate of genuine user is reduced thus improving FRR. For the improvement of FAR error rates, if the matching score is higher than the threshold, we resort to rechecking of the matching score to confirm the decision of imposter. As part of this rechecking if the matching score is greater than all the neighbourhood scores of the claimed identity then the user is authenticated as an imposter. On the other hand if the matching score is less than any one of neighbourhood scores of the claimed identity then the user is authenticated as genuine. In this way FAR is improved. The whole process by which FARs and FRRs are refined by using

the neighbourhood information is termed as refined score (RS) method.

## 3. EXPERIMENTAL RESULTS

We have extracted DAISY descriptor of FKP<sup>14-15</sup> as given in Appendix-A. Mittal<sup>16</sup>, *et al.* have utilised the same for the authentication of FKP<sup>14-15</sup>. FKP is first resized to 60x110 pixel resolution before applying DAISY descriptor on it. Only 14 points have been selected with ( $x=15:30:55$ ) and ( $y=15:15:110$ ) for the Daisy descriptor. The results of this descriptor are given in Table 1 for both training to test ratios of 5:1 and 6:6. The results are degraded as the number of test samples is increased in the latter as expected. The right middle finger gives the best genuine acceptance rate (GAR) of 97 per cent for the training to test ratios of 5:1 from DAISY descriptor at FAR of 0.01 per cent. The scores from individual FKPs are integrated by the sum rule giving rise to GARs of 99.5 per cent at FAR of 0.01 per cent using DAISY descriptor.

**Table 1. Results of DAISY descriptor (image size [60 110] points) per centGAR @ 0.01 per cent FAR**

FKP	DAISY DESCRIPTOR	
	TRAIN:TEST- 5:1	TRAIN:TEST-6:6
Left index	95.8	64.5
Left middle	95.15	71.4
Right index	96.4	68.6
Right middle	97	72.1
Score level fusion FKPs (sum rule)	99.5	91.8

Training set is used for learning while the test set is used to assess the performance of classifier. Here we have a fixed training set but the test set is changed for the evaluation of the performance of features.

Results from the GSHP response for all FKPs are shown in Table 2, while the results from the GSOD are shown in Table 3. The filter size is taken as 7x7 and the standard deviation as  $\sigma = 0.4$ . Table 4 gives the results of toposy and fractal dimension for the training to test ratio of 6:6.

**Table 2. GSHP (filter size 7x7,  $\sigma=0.4$ ), on FKP per centGAR @ 0.01 per cent FAR**

FKP	GSHP	
	Train:test-5:1	Train:test-6:6
Left index	98.8	79.2
Left middle	97	78.2
Right index	98.8	78.3
Right middle	99.4	85.3
Sum Rule	100	91

Figures 3(a) and 3(b), and Figs. 4(a), 4(b) show the comparative performance of DAISY descriptor and of GSHP on individual FKPs and their fusion at the score level using the sum rule for the training to test ratios of 5:1 and 6:6, respectively. Figures 5(a) and 5(b) illustrate the Receiver operating characteristics (ROCs) of individual FKPs on GSOD

**Table 3. Results from GSOD (filter size 7x7,  $\sigma = 0.4$ ) on FKP per centGAR @ 0.01 per cent FAR**

GSOD								
Orientation	Train:test-5:1				Train:test-6:6			
	Left index	Left middle	Right index	Right middle	Left index	Left middle	Right index	Right middle
$\pi/6$	98.2	96.9	97.5	99.4	59.3	74.3	66.3	73.8
$2\pi/6$	96.9	96.9	96.9	100	64.1	72.1	61.5	66.6
$3\pi/6$	96.9	95.7	98.7	99.8	55.3	61.8	59	61.8
$4\pi/6$	96.3	96.9	98.8	99.4	61	66	62	71.6
$5\pi/6$	96.9	97.1	99.4	100	61.4	74.3	67.1	74.3
$\Pi$	96.9	96.5	98.2	98.7	63	72.5	67	77.5
Sum rule	97.5	98.2	99	100	68.2	77.4	72.5	77.4

**Table 4. Results of fractal dimension and topothesy (6:6) per centGAR @ 0.01 per cent FAR**

Window size	Left index	Left middle	Right index	Right middle
5x5	86.2	90.8	87.8	92.8
6x6	85.8	90.8	88.3	92.1
7x7	82.5	89.8	88.5	90.4

features for the training to test ratios of 5:1 and 6:6. Figures 6(a) and 6(b) exhibit the performance of topothesy and fractal dimension without and with RS.

**4. COMPARISON WITH THE EXISTING METHODS**

Table 5 shows the comparison of results of different methods on the basis of per cent equal error rate (EER) and the number of genuine and imposter scores. The results of Compcode, ImpCompCode and MagCode on authentication of FKPs are taken directly from<sup>2</sup>. For each type of FKPs, each gallery or probe image contains 165 classes and 990 (165x6) sample images. If we take minimum of 6 scores from a test sample and 6 from a training sample, 990 genuine and 162360 (165x164x6) imposter matching scores are obtained. The actual numbers of genuine and imposter matching scores are 5940(165x6x6) and 974160(165x164x6x6) respectively. The results due to fractal parameters are the best when we use less number of genuine and imposter scores, i.e. 990 and 162360 for the image size of 0.5. On the other hand the results deteriorate with 5940 scores

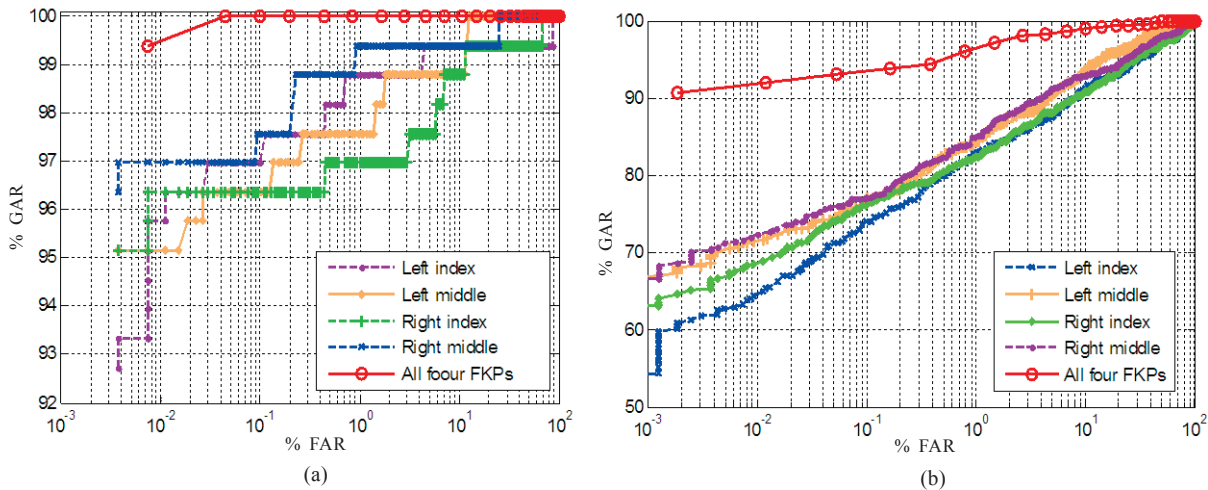


**Figure 3. ROCs of DAISY descriptor on individual FKPs and their fusion at score level using sum rule with training to test ratio (5:1), (6:6).**

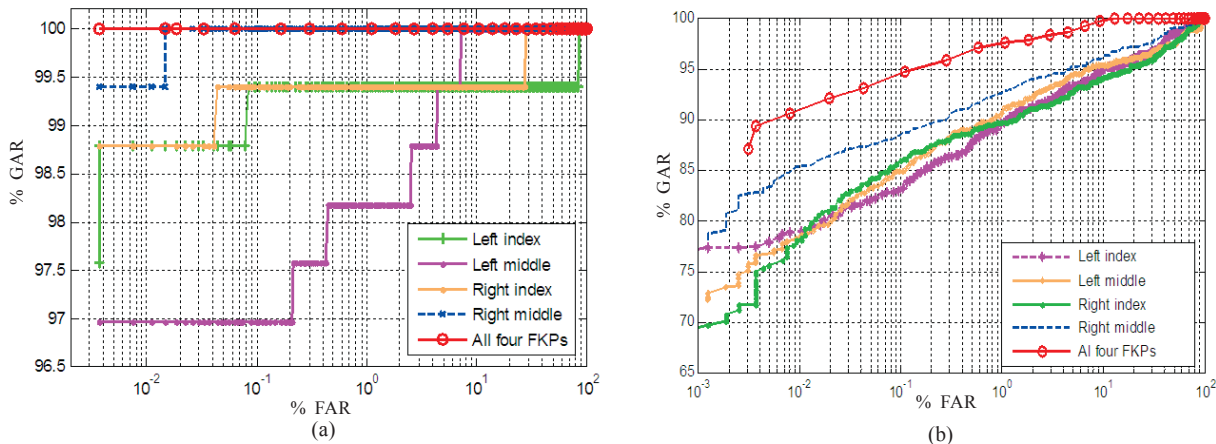


**Figure 4. ROCs of GSHP on the individual FKPs and their fusion at score level using sum rule with training to test ratio (5:1), (6:6).**

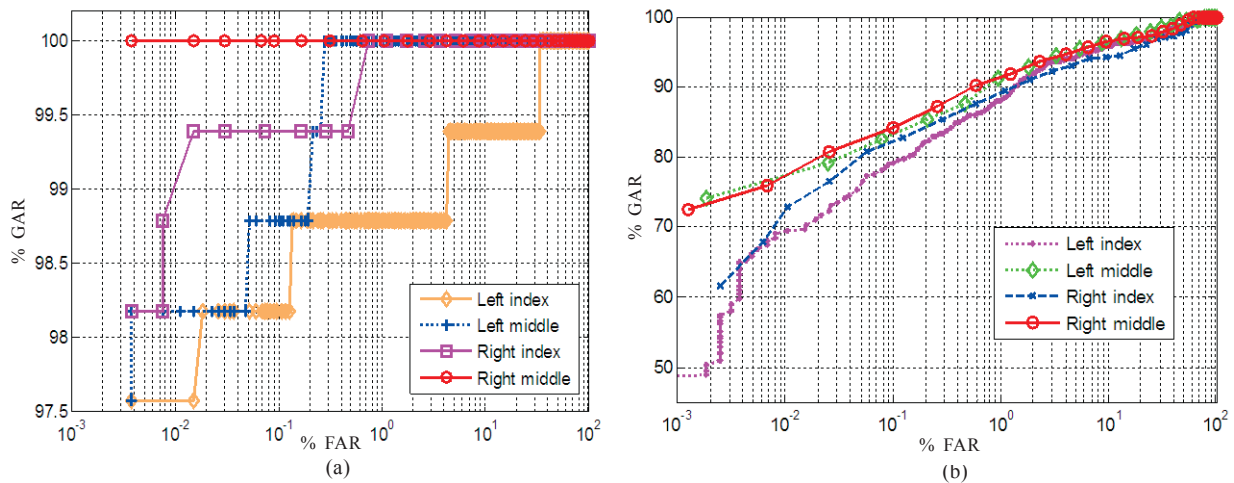


Figure 5. ROCs of GSOD on the individual FKPs with training to test ratio ((a) 5:1, (b) 6:6).

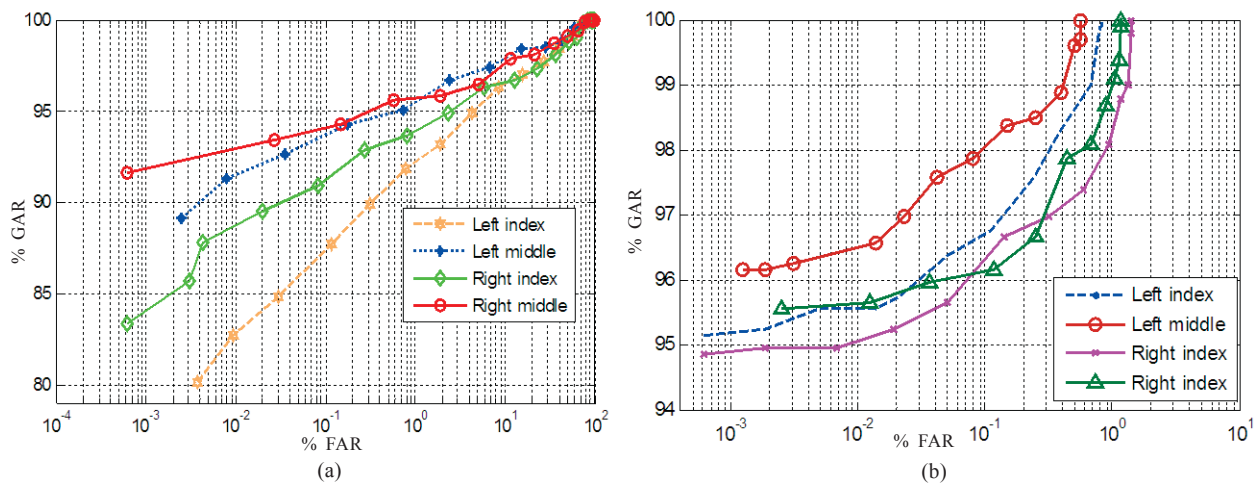


Figure 6. ROCs of topothesy and fractal dimension on the individual FKPs training to test ratio 6:6((a)without and (b)with RS).

Table 5. EERs (per cent) by different methods (6:6)

	Compcode (Zhang <sup>2</sup> , <i>et al.</i> )	ImpCompCode and MagCode (Zhang <sup>2</sup> , <i>et al.</i> )	(Topothesy + fractal dimension) RS based score level Window size 5x5 pixels		
			Image size 0.5	Image size 0.5	Image size 0.35
Number of genuine and imposter scores	5940, 487080	5940, 487080	990, 162360	5940, 974160	5940, 974160
Left index	2.06	1.73	0.46	4.68	3.47
Left middle	1.96	1.78	0.46	2.81	2.36
Right index	1.82	1.44	1.07	4.59	3.2
Right middle	1.87	1.64	0.93	3.68	2.85

with this image size. However by reducing the image size to 0.35 but keeping the same number of scores the results are improved and the feature dimension is reduced. These results are comparable to those due to CompCode, ImpCompCode and MagCode reported in the literature<sup>2</sup> on the basis of number of genuine and imposter scores.

### 5. CONCLUSIONS

In this work the FKP based authentication is presented. Two new features called GSHP and GSOD are implemented on FKPs. The existing DAISY descriptor, topothesy and fractal dimension together called fractal parameters are also

implemented on FKPs. The fractal parameters along with the refined scores provide the best results among all the methods implemented in this paper. The superior performance of fractal parameters is due to their ability to represent the texture effectively. Our results of FKP based authentication by fractal parameters are found to be comparable to those in the literature obtained using CompCode, ImpCompCode and MagCode. Thus the applicability of fractal parameters to the representation of the texture of FKPs is demonstrated and is a significant contribution of this paper. Further work is to extend GSHP features in the framework information set theory.

## REFERENCES

1. Zhang, Lin; Zhang, Lei & Zhang, David. Finger-knuckle-print: A new biometric identifier. *In* IEEE International Conference on Image Processing, Cairo, Egypt, 7-10 Nov 2009, 1981-1984. doi: 10.1109/icip.2009.5413734
2. Zhang, Lin; Zhang, Lei; Zhang, David & Zhu, Hailong. Online finger knuckle- print verification for personal authentication. *Pattern Recognition*, 2010, **43**(7), 2560-2571. doi: 10.1016/j.patcog.2010.01.020
3. Zhang, Lin; Zhang, Lei; Zhang, David & Zhu, Hailong. Ensemble of local and global information for finger knuckle print recognition. *Pattern Recognition*, 2011, **44**(9), 1990-1998. doi: 10.1016/j.patcog.2010.06.007
4. Zhang, Lin; Zhang, Lei; Zhang, David & Guo, Zhenhua. Phase congruency induced local features for finger-knuckle-print recognition. *Pattern Recognition*, 2012, **45**(7), 2522-2531. doi: 10.1016/j.patcog.2012.01.017
5. Morales, A.; Travieso, C.M.; Ferrer, M.A. & Alonso, J.B. Improved finger-knuckle-print authentication based on orientation enhancement. *Electronics Letters*, 2011, **47**(6), 380-381. doi: 10.1049/el.2011.0156
6. Zhu, Le-Qing. Finger knuckle print recognition based on SURF algorithm. *In* Proceedings of 8th International Conference on Fuzzy Systems and Knowledge Discovery, Shanghai, China, 26-28 July 2011, **3**, 1879-1883. doi: 10.1109/fskd.2011.6019781
7. Shariatmadar, Zahra S. & Faez, Karim. An efficient method for finger-knuckle-print recognition based on information fusion. *IEEE International Conference on Signal and Image Processing Applications (ICSIPA2011)*. doi: 10.1109/icsipa.2011.6144103
8. Militký, J. & Bajzík, V. Surface roughness and fractal dimension. *J. Textile Institute*, 2001, **92**(3), 91-113. doi: 10.1080/00405000108659617
9. Finger-Knuckle-print database. Biometric Research Center, H.K. Polytechnic University. Website <http://www4.comp.polyu.edu.hk/~biometrics/>. (Accessed on 28, July 2012)
10. Mamta & Hanmandlu, M. Multimodal biometric system built on the new entropy function for feature extraction and the refined scores as a classifier. *Expert Sys. Appl.*, 2015, **42**(2), 3702-3723. doi:10.1016/j.eswa.2014.11.054
11. Chaudhuri, B.B. & Sarkar, N. Texture segmentation using fractal dimension. *IEEE Trans. Pattern Anal. Mach. Intell.*, 1995, **17**(1), 72-77. doi: 10.1109/34.368149
12. Srinivasn, K.; Dastor, P.H.; Radhakrishnaiah, P. & Jayaraman, S. FDAS: A knowledge-based frame detection work for analysis of defects in woven textile structures. *J. Text. Inst.*, 1992, **83**(3), 431-447. doi: 10.1080/00405009208631217
13. Hanmandlu, M.; Chaudhary, D. & Das, S. Detection of defects in fabrics using topothesy fractal dimension features. *Signal, Image Video Proces.*, 2015, **9**(7), 1521-1530. doi: 10.1007/s11760-013-0604-5
14. Tola, Engin; Lepetit, Vincent & Fua, Pascal. DAISY: An efficient dense descriptor applied to wide base line stereo. *IEEE Trans. Pattern Anal. Mach. Intell.*, 2010, **32**(5), 815-830. doi: 10.1109/TPAMI.2009.77
15. Tola, Engin; Lepetit, Vincent & Fua, Pascal. A fast local descriptor for dense matching. *In* Proceedings of Computer Vision and Pattern Recognition, Anchorage, Alaska, USA, 23-28 June 2008, pp.1-8. doi: 10.1109/cvpr.2008.4587673
16. Mittal N.; Hanmandlu, M. & Vijay, R. A finger-knuckle-print authentication system based on DAISY descriptor. *In* 12<sup>th</sup> International Conference on Intelligent Systems Design and Applications (ISDA), 2012, 126-130. doi: 10.1109/isda.2012.6416524

## CONTRIBUTORS

**Dr Madasu Hanmandlu**, received the BE (Electrical Engg.) from Osmania University, Hyderabad, India in 1973, the MTech (Power Systems) from R.E.C. Warangal, Jawaharlal Nehru Technological University (JNTU), India, in 1976, and the PhD (Control Systems) from Indian Institute of Technology, Delhi, India, in 1981. From 1980 to 1982, he was a Senior Scientific Officer in Applied Systems Research Program (ASRP) of the Department of Electrical Engineering, IIT Delhi. His research interest include: Soft computing, machine learning, image processing and biometrics.

In the current study, he includes the help rendered in implementing the extraction of fractal parameters from FKP images and in writing the paper.

**Ms Neha Mittal**, received BTech (Electrical and Electronics Engineering) in 2004, MTech (Digital Communication) in 2010. She joined JP Institute of Engg. & Tech. as Senior Lecturer in 2010. Her research interest includes digital image processing and biometrics.

His contribution in the current study in includes the proposition of GSOD & GSHP features and comparison of three feature types (fractal parameters, GSOD & GSHP) with the CompCode, ImpCompCode and MagCode

**Dr Ritu Vijay**, received MSc and PhD in Electronics. She is working as Head & Associate Professor at Banasthali Vidhyapeeth, Banasthali, Rajasthan. Her areas of specialisation includes: Image and signal processing, embedded systems, wavelets and ANN.

In the current study, she includes the help in procuring the data of FKP, in implementing the features and in correcting the paper.

## Appendix A

### DAISY Descriptor

This descriptor due to Tola<sup>14,15</sup>, *et al.* is used to extract daisy features from palmprints. An image may belong to any one of four spectral bands. For a given input image  $I$ , eight orientation maps  $G_i$  are computed, one for each quantised direction. If direction is greater than zero  $G_o(u, v)$  equals the image gradient norm at location  $(u, v)$ , else it is zero. The maps that preserve polarity of the intensity changes are defined as

$$G_o = \left( \frac{\partial I}{\partial o} \right)^+ \quad (\text{A.1})$$

where  $(\cdot)^+$  is the operator such that  $(a)^+ = \max(a, 0)$ . The convolved orientation maps are obtained by convolving orientation maps with the Gaussian kernels  $G_\Sigma$  for various  $\Sigma$ .

$$G_o^\Sigma = G_\Sigma * \left( \frac{\partial I}{\partial o} \right)^+ \quad (\text{A.2})$$

For instance,  $G_o^{\Sigma_2}$  can be computed with  $\Sigma_2 > \Sigma_1$  as

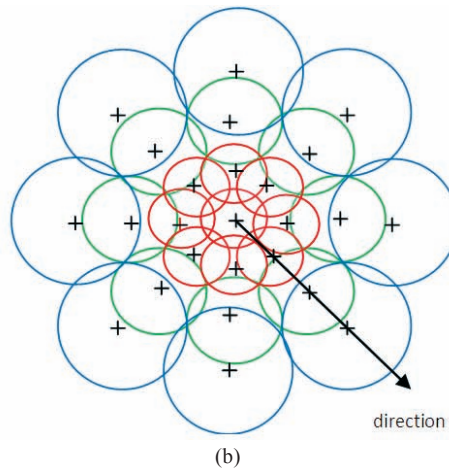
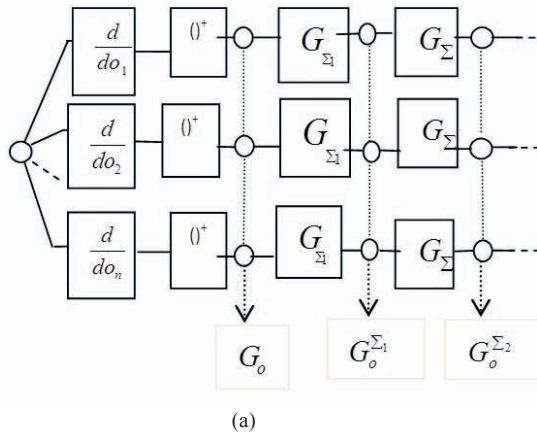
$$G_o^{\Sigma_2} = G_{\Sigma_2} * \left( \frac{\partial I}{\partial o} \right)^+ = G_{\Sigma_2} * G_{\Sigma_1} * \left( \frac{\partial I}{\partial o} \right)^+ = G_{\Sigma_2} * G_o^{\Sigma_1} \quad (\text{A.3})$$

For an input image  $I$ , the convolution of the orientation maps is shown in Fig. A1(a). DAISY descriptor at a particular pixel consists of the convolved orientation maps located on the concentric circles and the radii of the circles and the amount of Gaussian smoothing are proportional to each other. As this descriptor appears like a flower, it is named as Daisy shown in Fig. A1(b).

Let  $h_\Sigma(u, v)$  be the vector consisting of convolved orientation maps at location  $(u, v)$  where  $\Sigma$  is the standard deviation. It is denoted by

$$h_\Sigma(u, v) = [G_1^\Sigma(u, v), \dots, G_8^\Sigma(u, v)]^T \quad (\text{A.4})$$

where  $G_1^\Sigma, G_2^\Sigma$  and  $G_8^\Sigma$  are the convolved orientation maps in 8 different directions. This vector is normalised to unit norm denoted by  $\tilde{h}_\Sigma(u, v)$ . Each histogram is normalised independently. The DAISY descriptor  $D(u_o, v_o)$  for three



circular layers,  $Q=3$  at location  $(u_o, v_o)$  consists of the following concatenated  $\tilde{h}$  vectors:

$$D(u_o, v_o) = [\tilde{h}_{\Sigma_1}^T(u_o, v_o), \tilde{h}_{\Sigma_1}^T(I_1(u_o, v_o, R_1)), \dots, \tilde{h}_{\Sigma_1}^T(I_N(u_o, v_o, R_1)), \tilde{h}_{\Sigma_2}^T(I_1(u_o, v_o, R_2)), \dots, \tilde{h}_{\Sigma_2}^T(I_N(u_o, v_o, R_2)), \tilde{h}_{\Sigma_3}^T(I_1(u_o, v_o, R_3)), \dots, \tilde{h}_{\Sigma_3}^T(I_N(u_o, v_o, R_3))]^T \quad (\text{A.5})$$

where  $I_j(u, v, R)$  is location in the direction  $j$  with distance  $R$  from pixel  $(u, v)$ . Here 8 directions and 3 concentric circles so the descriptor contains  $8 \times 8 \times 3 \times 8 = 200$  values from 25 locations and 8 orientations have been used.

This descriptor is also resistant to rotational variations because it is constructed from an isotropic Gaussian kernel merged with a circular grid. The overlapping regions ensure a smoothly changing descriptor along the rotation axis and it can be made more robust up to the point where the descriptor starts losing its discriminative power on increasing the overlap. The daisy descriptor calculated from palmprint is shown in Fig. A2.

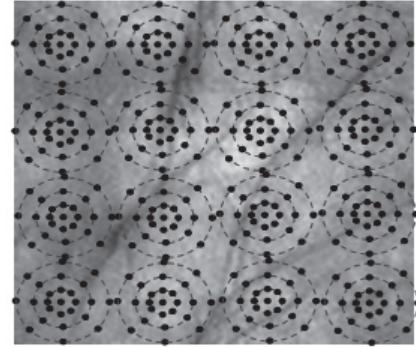


Figure A2. Daisy descriptor calculated from palmprint.

Figure A1. (a) The computation of the orientation maps of given image and the convolution of the orientation maps. (b) Daisy descriptor: the radius of each circle is proportional to the standard deviation of the Gaussian kernel.